Available online at www.sciencedirect.com
SCIENCE DIRECT®
Biochemical Pharmacology 67 (2004) 1167–1184
Biochemical Pharmacology
www.elsevier.com/locate/biochempharm

Effects of enhancing mitochondrial oxidative phosphorylation with reducing equivalents and ubiquinone on 1-methyl-4-phenylpyridinium toxicity and complex I–IV damage in neuroblastoma cells

Elizabeth A. Mazzio, Karam F.A. Soliman*

College of Pharmacy and Pharmaceutical Sciences, Florida A&M University, Tallahassee, FL 32307, USA

Received 17 September 2003; accepted 13 November 2003

Abstract

The effects of increasing mitochondrial oxidative phosphorylation (OXPHOS), by enhancing electron transport chain components, were evaluated on 1-methyl-4-phenylpyridinium (MPP+) toxicity in brain neuroblastoma cells. Although glucose is a direct energy source, ultimately nicotinamide and flavin reducing equivalents fuel ATP produced through OXPHOS. The findings indicate that cell respiration/mitochondrial O_2 consumption (MOC) (in cells not treated with MPP+) is not controlled by the supply of glucose, coenzyme Q_{10} (Co-Q_{10}), NADH+, NAD or nicotinic acid. In contrast, MOC in whole cells is highly regulated by the supply of flavins: riboflavin, flavin adenine dinucleotide (FAD) and flavin mononucleotide (FMN), where cell respiration reached up to 410% of controls. In isolated mitochondria, FAD and FMN drastically increased complex I rate of reaction (1300%) and (450%), respectively, having no effects on complex II or III. MPP+ reduced MOC in whole cells in a dose-dependent manner. In isolated mitochondria, MPP+ exerted mild inhibition at complex I, negligible effects on complexes II–III, and extensive inhibition of complex IV. Kinetic analysis of complex I revealed that MPP+ was competitive with NADH, and partially reversible by FAD and FMN. Co-Q_{10} potentiated complex II (~200%), but not complex I or III. Despite positive influence of flavins and Co-Q_{10} on complexes I–II function, neither protected against MPP+ toxicity, indicating inhibition of complex IV as the predominant target. The nicotinamides and glucose prevented MPP+ toxicity by fueling anaerobic glycolysis, evident by accumulation of lactate in the absence of MOC. The data also define a clear anomaly of neuroblastoma, indicating a preference for anaerobic conditions, and an adverse response to aerobic. An increase in CO_2, CO_2/O_2 ratio, mitochondrial inhibition or O_2 deprivation was not directly toxic, but activated metabolism through glycolysis prompting depletion of glucose and starvation. In conclusion, the results of this study indicate that the mechanism of action for MPP+ involves the inhibition of complexes I and IV, leading to impaired OXPHOS and MOC. Moreover, the results also indicate that flavin derivatives control the rate of complex I and more specifically complex IV, leading to impaired OXPHOS and MOC.

Keywords: MPP+; Parkinson's disease; Riboflavin; Coenzyme Q; Complex IV; ATP

1. Introduction

The pathogenesis of Parkinson's disease (PD) involves targeted degeneration of nigrostriatal dopaminergic neurons. An extensive body of research suggests that mitochondrial mutations or environmental exposure to mitochondrial toxins such as herbicides and pesticides may play a predominant role in disease etiology [1,2]. In neurons, the loss of mitochondrial function can lead to abnormal glucose oxidation and a loss of energy (ATP) derived through OXPHOS. Moreover, abnormal glucose oxidation patterns are inherent to several degenerative CNS diseases such as Alzheimer's disease, dementia, schizophrenia and other psychoses [3].

* Corresponding author. Tel.: +1-850-599-3306; fax: +1-850-599-3667.
E-mail address: karam.soliman@famu.edu (K.F.A. Soliman).

Abbreviations: AB, almar blue; ATP, adenosine-5′-triphosphate; CNS, central nervous system; CO_2, carbon dioxide; Co-Q_{10}, coenzyme-Q_{10}; DCPIP, 2,6-dichlorophenolindophenol; DMEM, Dulbecco's modified Eagle medium; EDTA, ethylenediaminetetraacetic acid; EGTA, ethylene glycol-bis(β-aminoethyl ether)-*N*,*N*,*N*′*N*′-tetraacetic acid; ETC, electron transport chain; FAD, flavin adenine dinucleotide; FMN, flavin mononucleotide; H_2O, water; HBSS, Hank's balanced salt solution; HEPES, (*N*-2-hydroxyethylpiperazine-*N*′-[2-ethanesulfonic acid]); HPLC, high performance liquid chromatography; KCl, potassium chloride; MOC, mitochondrial oxygen consumption; MPP+, 1-methyl-4-phenylpyridinium; MPTP, 1-methyl-4-phenyl-1,2,3,6-tetrahydropyridine; MTT, 3-(4,5-dimethylthiazol-2-yl)-2,5-diphenyltetrazolium bromide; NaCl, sodium chloride; NADH, nicotinamide adenine dinucleotide—reduced form; O_2, oxygen; OXPHOS, oxidative phosphorylation; PBS, phosphate-buffered saline; PD, Parkinson's disease.

0006-2952/$ – see front matter © 2004 Elsevier Inc. All rights reserved.
doi:10.1016/j.bcp.2003.11.016

In PD, the dysfunction of NADH-ubiquinone oxidoreductase (complex I) has been the focus of many studies. Mitochondrial DNA mutations and biochemical defects, specific to mitochondrial complex I, were manifested in confirmed PD cases [1,4,5]. *In vivo*, chronic exposure to rotenone and specific complex I inhibitors, can reproduce the biochemical and pathological features of PD. Furthermore, the administration of complex I inhibitors can enhance the formation of localized alpha-synuclein aggregates, increase reactive oxygen species, stimulate apoptosis and prompt targeted destruction of dopaminergic nigral neurons [6–8]. The neurotoxin MPTP causes PD pathology in humans and primates, through the direct action of MPP+ on complex I inhibition [9]. Similarly, endogenously produced toxins structurally similar to MPP+ such as 1-benzyl-1,2,3,4-tetrahydroisoquinoline [10], *N*-methyl-(*R*)-salsolinol [11,12] and 5-*S*-cysteinyl-dopamine/7-(2-aminoethyl)-3,4-dihydro-5-hydroxy-2*H*-1,4-benzothiazine-3-carboxylic acid [13] are believed to mediate targeted nigral damage through complex I inhibition.

While the effects of MPP+ on complex I have been the focus of many studies, there are several conceptual concerns observed. First, is the reported high concentrations of MPP+ required to moderately inhibit complex I activity, up to 10 mM [14–16], indicating its weakness as an inhibitor. These findings suggest that MPP+ may contribute to mitochondrial dysfunction through another mechanism. Second, Co-Q_{10} is currently under clinical investigation for therapeutic use in PD [17]. However, the effects of Co-Q_{10} on complex I, with regards to MPP+ are not clearly understood. Complex I transfers electrons, from NADH to Co-Q_{10}, and translocates protons across the inner mitochondria, indicating its role is downstream to the catalytic activity of complex I, the target of MPP+. Likewise, pilot studies in our lab, have indicated that Co-Q_{10} does not appear to increase the V_{max} or reduce the K_m of complex I, but exerts kinetic effects on complex II. However, complex II is not a known target of MPP+. Other studies have reported similar intrinsic affinity of Co-Q_{10} for complex II activity rather than complex I [18]. Lastly, the cytoprotective effects of glucose against MPP+ in neuroblastoma cells reportedly occur through sustaining anaerobic glycolysis, without reversing mitochondrial impairment as demonstrated by a sustained block in cell O_2 consumption [19]. However, increased viability is observed during glucose protection against MPP+ using MTT [20]. MTT detects viability by measuring mitochondrial NADH oxidoreductase (complex I) activity, a synonymous target of MPP+. However, an increase of MTT cleavage during cytoprotection with glucose is observed even when mitochondrial function is completely blocked by MPP+ [19–21]. These findings suggest that MPP+ inhibits the mitochondria downstream to complex I, or that MTT detects viability primarily through cytosolic dehydrogenase enzymes. Furthermore, the incongruent nature of MTT and MPP+ on complex I, questions the validity of this method for *in vitro* toxicology models, where ATP can be produced by anaerobic substrate level phosphorylation. Therefore, the current investigation was designed to elucidate the specific effects of MPP+ on complexes I–IV activity in isolated mitochondria and whole cells. In addition, the cytoprotective role of ergogenic compounds against MPP+ toxicity through aerobic and anaerobic survival responses were examined.

2. Materials and methods

2.1. Materials

Murine brain neuroblastoma cells (N-2A cells) were obtained from American Type Culture Collection. DMEM, L-glutamine, fetal bovine serum-heat inactivated (FBS), HBSS, PBS and penicillin/streptomycin were supplied by Fischer Scientific, Mediatech. MPP+, H_2SO_4, coenzyme Q_{10} and all other chemicals and supplies were purchased from Sigma Chemical Co.

2.2. Cell culture

N-2A cells exhibit neuronal brain morphology, display vast neurite extensions and adhere to plastic. Moreover, these cells are vulnerable to MPP+, oxygen radical species and catecholamines [19–22]. In addition, previous studies in our laboratory have established that N-2A cells are more vulnerable to the toxic effects of MPP+ than rat PC-12 and human SH-SY5Y cells, when glucose and cell densities are controlled. In the current study, N-2A cells were grown in DMEM containing phenol red, 10% FBS (v/v), 4 mM L-glutamine, penicillin (100 U/mL)/streptomycin (0.1 mg/mL) and 20 μM of sodium pyruvate. Cells were cultured and maintained at a temperature of 37° and 5% CO_2/atmosphere. The cells were gently scraped and subcultured every 2–5 days. The experimental media consisted of DMEM (without phenol red), supplemented with 1.8% FBS (v/v), penicillin (100 U/mL)/streptomycin (0.1 mg/mL), 4 mM L-glutamine and 20 μM sodium pyruvate. For experiments, cells were plated at approximately 0.5×10^6 cells/mL in 96-well plates. A stock solution of each experimental compound was prepared in HBSS containing 5 mM HEPES, adjusted to a pH of 7.4. In each experiment, six concentrations of each treatment were prepared to span a 1000-fold dilution range. Pure Co-Q_{10} was dissolved in hot corn oil and acetic acid, followed by sonication and emulsification into a semi-gel. In order to ensure accuracy of the findings, results were compared to those acquired using a commercially available hydrosoluble Co-Q_{10} formulation with superior bioavailability Q-Gel® (Tishcon Corp.). Solutions of MPP+ were prepared fresh daily in buffered HBSS.

2.3. Cell viability

Almar blue (AB) indicator dye was used to assess cell viability. AB fluorescence detection constitutes a rapid, reliable and sensitive method to examine toxicity [23]. In this study, a working solution of resazurin (0.5 mg/mL) was prepared in sterile PBS. The dye solution was added, 15% (v/v) equivalent to the samples, and incubated for 6–12 hr. Live, MPP+ and blank controls were run on each plate with experimental treatments to avoid interference or interplate variability. Quantitative analysis of dye conversion was measured on a microplate fluorometer—Model 7620-version 5.02, Cambridge Technologies Inc. with settings fixed at (550/580) (excitation/emission), wavelengths.

2.4. Lactic acid determinations

Lactic acid was quantified by HPLC consisting of an Interaction Ion-300 anion exchange column on a Waters 2487/Millennium 32 version 3.20, system controller with 2690 Separations Module and UV detector (210 nm). The mobile phase consisted of 0.01 N H_2SO_4, the flow rate was set at 0.4 mL/min and column temperature 40°.

2.5. Dissolved O_2 and atmospheric CO_2/O_2 measurements

Whole cell mitochondrial O_2 consumption was analyzed using a Clark electrode (Hansatech Instruments Ltd.). The electrode quantifies dissolved O_2 in the medium as a means to assess mitochondrial respiration. The electrode was calibrated with air saturated deionized water (air line) and deionized water containing sodium dithionite (nitrogen line). The samples or control blanks were loaded into the chamber jacket at 25°. After the instrument was stabilized and equilibrated, the raw data were acquired as nM of O_2/mL and converted to percentage of control values. Experiments altering the air concentration of CO_2/O_2 ratio were accomplished by injecting pure CO_2 into a closed chamber maintained at 37°. Gas ratios of CO_2/O_2 in the incubator, atmosphere and enclosed chambers were monitored using a digital Bacharach—Model 2835 CO_2 analyzer.

2.6. Glucose analysis

DMEM glucose was quantified after 12 hr of experimental treatments. Briefly, detection was acquired using an enzymatic assay as previously described [19,24]. The chromogen consisted of glucose oxidase (20 U/mL) and a final working concentration of 1 mM vanillic acid, 500 μM of 4-aminoantipyrine and 4-purpurogallin U/mL of horseradish peroxidase—type II prepared in distilled water + 10 mM HEPES, adjusted to a pH of 5.1. The combined reagent was added to each sample and returned to the incubator for 5 min at 37°. Glucose was quantified at 490 nm wavelength on a UV microplate spectrophotometer—Model 7520 version 5.02, Cambridge Technologies Inc. The glucose standard curve (0.01–10 mM) was prepared in buffered distilled water. The data were expressed as percentage of the control relative to the DMEM blank, without cells.

2.7. Measurements of mitochondrial respiratory chain activities

Mitochondria activities were determined using a modification of a previously described method [25,26]. In this method, N-2A cells were cultured, harvested, pelleted and washed in PBS prior to being dispersed in ice cold mitochondrial isolation buffer solution. The buffer solution consisted of HEPES (20 mM), pH 7.4, $MgCl_2$ (1.5 mM) KCl (10 mM), EDTA (1 mM), dithiothreitol (1 mM), EGTA (1 mM), phenylmethylsulfonyl fluoride (1 mM), leupeptin (10 μM), aprotinin (10 μM) and sucrose (250 mM). Cells were homogenized, chilled on ice for 3 min, disrupted and centrifuged at 500 *g* for 10 min at 4°. The mitochondria were pelleted by centrifugation at 9400 *g* for 10 min at 4°. The protein concentration of the mitochondrial homogenate was adjusted so that the final working concentration was equal to ∼200 μg/mL. Protein was determined with the Lowry *et al.* procedure and bovine albumin was used as a standard (0–100 mg/dL) [27]. Typically, protocols utilize reaction mixtures that are adjusted to a pH of 7.4. However, in method validation control studies, we found that in blastoma cells, mitochondrial complexes II–IV exhibited optimum activity at a pH of ∼5.6. This effect may be due to the unusual metabolism that enables immortal cell lines to thrive under acidic conditions. Moreover, the lower pH may have favored availability of H+ to potentiate the transfer of electrons.

2.8. Complex I determinations

NADH: ubiquinone oxidoreductase activity was determined by quantifying the decrease in UV absorbance that accompanied the oxidation of NADH at 340 nm. The reaction mixture consisted of sodium phosphate (8 mM), NaCl (136 mM), $CaCl_2$ (1 mM), HEPES (25 mM), $MgSO_4$ (10 mM) and KCl (2.5 mM) in deionized H_2O. The buffer contained 2.5 mg/mL bovine serum albumin, 50 μg/mL antimycin A, sodium azide 4 mM, 50 μM decylubiquinone, ±FAD 25 μM and FMN 25 μM. The final pH was re-adjusted to 7.4. The reactant solution was added to the mitochondrial homogenate and the reaction was initiated by the addition of 500 μM NADH. A standard curve was established for NADH along with an NAD+ non-response control (1–2500 μM). Experimental control blanks were run simultaneously to account for any interference or substrate interaction. Complex I activity was assessed in the presence of antimycin and sodium azide, but not malonate, as previous data in our laboratory have indicated that the addition of malonate up to 15 mM did not affect this reaction. Rotenone was used as a control in complex

I activity assays to specify rotenone sensitive NADH dehydrogenase activity.

2.9. Complex II determinations

Succinate-ubiquinone oxidoreductase activity was quantified by measuring the decrease in UV absorbance due to the reduction of DCPIP at 600 nm. The reaction mixture consisted of sodium phosphate (8 mM), NaCl (136 mM), $CaCl_2$ (1 mM), HEPES (25 mM), $MgSO_4$ (10 mM) and KCl (2.5 mM) in deionized H_2O. The buffer contained 2.5 mg/mL bovine serum albumin, 12 mM succinic acid, 50 μM decylubiquinone, ± (FAD 25 μM and FMN 25 μM), 75 μM DCPIP, 50 μg/mL antimycin A and sodium azide 4 mM. The final pH was re-adjusted to 5.6. The reactant solution was added to the mitochondrial homogenate and DCPIP reduction was monitored over time. A standard curve was established using DCPIP (1–100 μM) and experimental control blanks were run simultaneously to account for any interference or substrate interaction. Complex II was assessed in the presence of antimycin and sodium azide, which blocked the electron transfer through the cytochromes and enabled detection of complex II. Rotenone was not added in the quantification of complex II, because previous data from our laboratory have indicated that the activity measured in complex II was independent of complex I or addition of rotenone.

2.10. Complex III determinations

Ubiquinol: cytochrome *c* oxidoreductase was determined by monitoring the reduction of oxidized cytochrome *c* at 550 nm. The reaction mixture consisted of sodium phosphate (8 mM), NaCl (136 mM), $CaCl_2$ (1 mM), HEPES (25 mM), $MgSO_4$ (10 mM) and KCl (2.5 mM) in deionized H_2O. The reaction mixture contained 2.5 mg/mL bovine serum albumin, 12 mM succinic acid, 50 μM decylubiquinone, 4 mM sodium azide and 125 μM cytochrome *c*. The final pH was re-adjusted to 5.6. The reactant solution was added to the mitochondrial homogenate and reduction was monitored over time. The oxidation–reduction state of cytochrome *c* was established with ascorbic acid and experimental control blanks were run simultaneously to account for any interference or substrate interaction. For determination of complex III, unlike most studies, we used the succinate (15 mM) to drive complex II in the presence of 4 mM sodium azide, which blocked complex IV–cytochrome oxidase. This elicited a very large signal response in complex III, with activity completely reducing the oxidized cytochrome *c*.

2.11. Complex IV determinations

Cytochrome *c* oxidase was determined by monitoring the oxidation of reduced cytochrome *c* at 550 nm. The reaction mixture consisted of sodium phosphate (8 mM), NaCl (136 mM), $CaCl_2$ (1 mM), HEPES (25 mM), $MgSO_4$ (10 mM) and KCl (2.5 mM) in deionized H_2O. The reaction mixture contained 2.5 mg/mL bovine serum albumin, 50 μM decylubiquinone, 50 μg/mL antimycin and 15 mM malonate. Cytochrome *c* 125 μM was added in the presence of 3 mM ascorbic acid. The final pH was re-adjusted to 5.6. The reactant solution was added to the mitochondrial homogenate and oxidation was monitored over time. Experimental control blanks were run simultaneously to account for any interference or substrate interaction. A modification was essential for the detection of complex IV–cytochrome oxidase. Complex IV could not be assessed properly without the addition of malonate combined with antimycin, which brought on a near complete oxidation of the reduced cytochrome *c*. This indicates that it is crucial to inhibit all reductive capacity of the electron transport chain in order to properly test for cytochrome oxidase–complex IV. This is an interesting point, as most protocols and kits for determination of cytochrome oxidase, do not include complex II and III inhibitors, which may lead to a negligible signal or require extremely large amounts of homogenate.

2.12. Data analyses

Statistical analysis was performed using Graphpad Prism—version 3.0/Graphpad Software Inc. Data were expressed as the mean ± SEM for each group. Significance of difference between the groups was assessed using a one-way/two-way ANOVA, followed by a Tukey post hoc means comparison test.

3. Results

3.1. MPP+ toxicity

The effects of MPP+ at various concentrations (0, 0.01, 0.05, 0.1, 1, 5 and 10 mM) were evaluated to determine the effects on cell viability and mitochondrial respiration (Fig. 1A). The data presented in Fig. 1A show a decline in both parameters measured. Toxicity of MPP+ (500 μM) corresponded to accelerated glucose utilization and depletion, resulting in exhaustion of energy supplies in a glucose-limited environment (Fig. 1B). The following set of experiments corroborate that rapid consumption of glucose in the presence of MPP+, is the result of accelerated glycolysis that occurs as an anaerobic compensatory survival response.

3.2. Anaerobic glycolysis

Providing additional glucose or nicotinamides (0.01, 0.05, 0.1, 1, 5, and 10 mM), but not riboflavin protected against MPP+ (500 μM) toxicity (Fig. 1C). The addition of Co-Q_{10} did not protect against MPP+ toxicity (Fig. 1D)

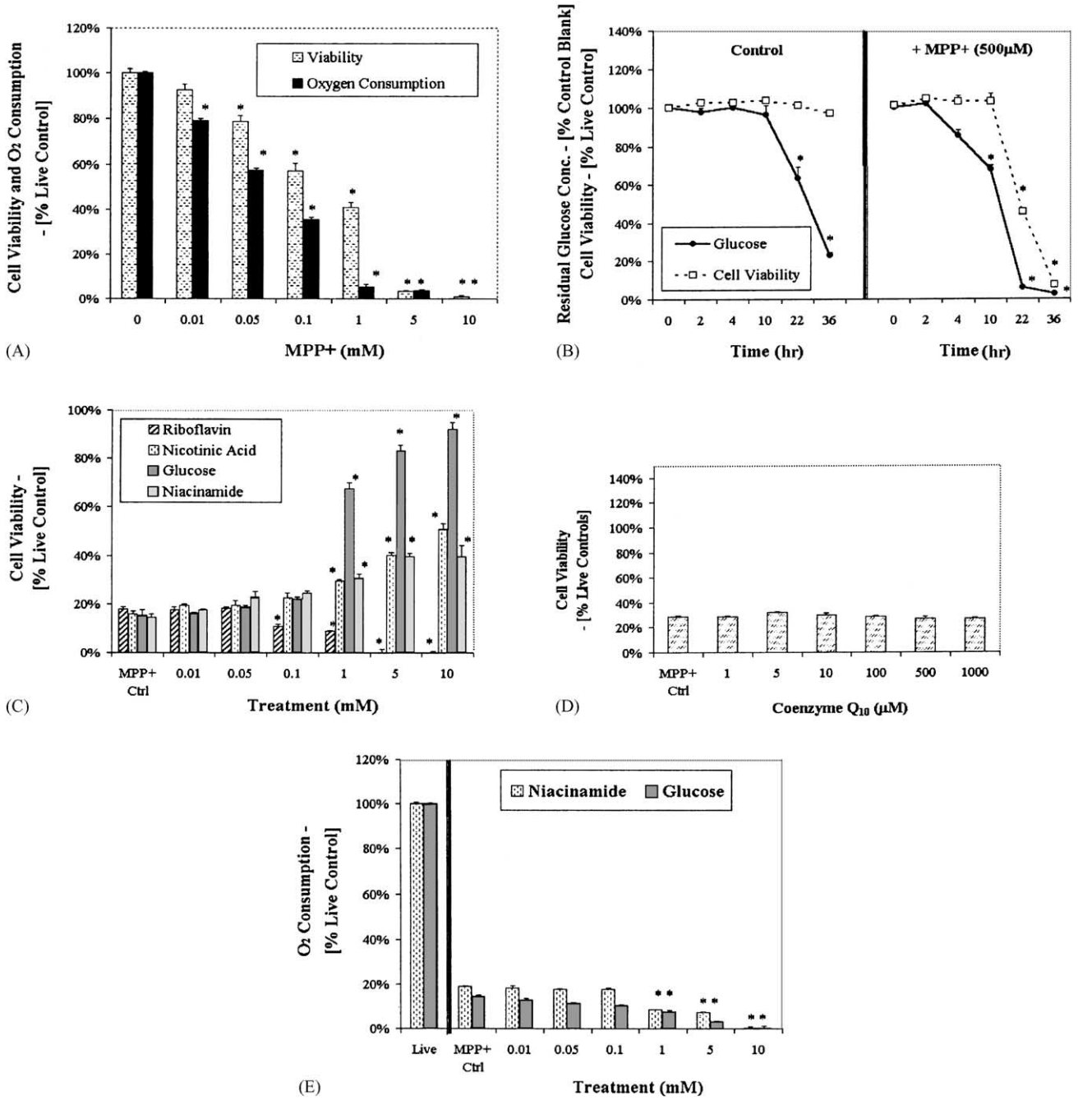

Fig. 1. (A) The effects of MPP+ on toxicity and O_2 consumption of N-2A cells at 24 hr. The data represent cell viability and cell O_2 consumption (as percent live controls) and are expressed as the mean ± SEM (N = 4). Significance differences from the live controls were determined by a one-way ANOVA, followed by a Tukey mean comparison post hoc test, $^*P < 0.001$. (B) Glucose consumption in baseline and MPP+ (500 μM) treated cells relative to toxicity over a 36 hr period. The data represent glucose concentration in the DMEM media, relative to a blank and cell viability as percent controls. The data are expressed as the mean ± SEM (N = 4) and the significance of difference from the T_0 controls were determined by a one-way ANOVA, followed by a Tukey mean comparison post hoc test, $^*P < 0.001$. (C) The cytoprotective effects of glucose, niacinamide, nicotinic acid and riboflavin (10 μM–10 mM) on MPP+ (500 μM) toxicity in N-2A cells. The data represent cell viability as percent of live controls and are expressed as the mean ± SEM (N = 4). The significance of difference from the MPP+ treated controls were determined by a one-way ANOVA, followed by a Tukey mean comparison post hoc test, $^*P < 0.001$. (D) The effects of Co-Q_{10} on MPP+ (500 μM) toxicity in N-2A cells. The data represent cell viability as percent of live controls and are expressed as the mean ± SEM (N = 4). The significance of difference from the MPP+ treated controls were determined by a one-way ANOVA, followed by a Tukey mean comparison post hoc test. There were no significant differences. (E) The effects of niacinamide and glucose (10 μM–10 mM) on mitochondrial O_2 consumption during cytoprotection against MPP+ (500 μM). The data represent O_2 consumption as percent of live untreated controls. The data are expressed as the mean ± SEM (N = 4). The significance of difference from the MPP+ treated controls were determined by a one-way ANOVA, followed by a Tukey mean comparison post hoc test, $^*P < 0.001$.

Table 1
Lactic acid produced in N-2A cells under normal conditions, treatment with MPP+ and during glucose rescue against MPP+

Group	DMEM glucose concentration (mM)	Lactic acid produced (mM at 24 hr)	
		Mean ± SE	
Blank	5.5	0.0 ± 0.1	Significant
Cells	5.5	8.7 ± 0.8	*
MPP+ (500 μM)	5.5	10.9 ± 1.4	*
MPP+ (500 μM) + 10 mM glucose	15.5	21.2 ± 2.1	*

The data represent lactic acid produced in untreated cells, cells treated with MPP+ (500 μM) and during glucose (10 mM) protection against MPP+. The result displays DMEM glucose concentration (mM) and lactate produced (mM) at 24 hr. The significance of difference from the control blank was determined by a one-way ANOVA, followed by a Tukey mean comparison post hoc test, $^{*}P < 0.001$.

with results similar at all concentrations. The cytoprotection by glucose and nicotinamide occurred without reversing the loss of mitochondrial O_2 consumption by MPP+ (Fig. 1E) and corresponded to an even larger decline in O_2 consumption. These data indicate that effects of glucose and niacinamide are likely due to their functional roles in fueling anaerobic glycolysis during mitochondrial impairment. The role of anaerobic glycolysis in overcoming the toxic effects of MPP+ is evident in Table 1. Table 1 demonstrates that N-2A cells normally produce abundant lactic acid from glucose in the medium. The addition of MPP+ (500 μM) caused a greater shift toward anaerobic glycolysis. And, cytoprotection by glucose (10 mM) in the presence of MPP+ (500 μM) augmented lactic acid production to extremely high levels in excess of 20 mM at 24 hr incubation. The high levels of lactate produced during complete loss of mitochondrial O_2 consumption as demonstrated in Fig. 1E, corroborate strict anaerobic glycolysis during cytoprotection.

Metabolic derivatives of riboflavin and nicotinamide play a critical role in aerobic energy function through the mitochondria. Therefore, we examined the protective effects of NADH+, FAD and FMN against MPP+ (500 μM) (Fig. 2A). Similar to the precursor compounds, only NADH+, but not FAD and FMN provided partial protection. And, the cytoprotection by NADH+ corresponded to a drop in O_2 consumption, indicating protective effects were the result of potentiating lactic acid dehydrogenase rather than mitochondrial NADH+ dehydrogenase (Fig. 2B).

3.3. Regulation of mitochondrial O_2 consumption

Energy compounds were examined for regulatory influence on aerobic cell respiration by monitoring mitochondrial O_2 consumption in the absence of MPP+ (Fig. 2C–E). Figure 2C and D demonstrate that supply of glucose, niacinamide, Co-Q_{10}, NADH and NAD+ do not control the rate of cell respiration. On the other hand, Fig. 2C demonstrates a significant role for riboflavin in controlling cellular O_2 consumption. The obvious pattern of cell death induced by riboflavin is a critical issue, and will be discussed later in the paper. Figure 2E corroborates that riboflavin derivatives: FAD and FMN exert powerful influence on cell O_2 consumption, where rate of cell respiration reaches up to 410% of controls.

3.4. Complex I

In order to examine the mechanism by which the flavins control rate of cell respiration, studies were preformed on mitochondrial isolates. FMN and FAD drastically increased the velocity of complex I in isolated mitochondria, in a very similar pattern to effects on whole cell mitochondrial O_2 consumption (Fig. 3A and B). Due to the powerful effects of FAD and FMN on complex I reaction rate, both were added to the reactant solution for subsequent experiments. A control for complex I activity in the presence of flavin derivatives was established by monitoring NADH oxidation over time (Fig. 3C). Figure 3D displays complex I activity over time in the presence of rotenone (100 μM, 500 μM and 1 mM). These data indicate rotenone to be a weak inhibitor of complex I. Similarly, the effects of MPP+ on complex I activity were mild as determined by holding the substrate constant (500 μM NADH) with varying MPP+ concentration (Fig. 3E) and varying NADH concentrations, holding (MPP+ 1 mM) constant (Fig. 3F). Co-Q_{10} had no effect on complex I activity alone (left panel) and did not reverse the inhibitory effects of MPP+ (right panel) (Fig. 3G). Kinetic analysis indicated that MPP+, mildly attenuated complex I activity in a non-competitive fashion in the presence of FAD and FMN, and acted competitive with the substrate, NADH (Fig. 3H).

3.5. Complex II

A timed control for complex II activity was established, monitoring the reduction of DCPIP from 0 to 180 min (Fig. 4A). Complex II specific activity was validated by inhibition with malonate (150 μM–15 mM) over 60 min (Fig. 4B). Malonate (15 mM) was a potent inhibitor and 100% effective in inhibiting complex II activity. Co-Q_{10} increased complex II activity, while nicotinamide and flavin reducing equivalents had no effect (Fig. 4C). Moreover, MPP+ (10 mM) induced a very mild inhibition of complex II activity (Fig. 4D).

3.6. Complex III

A timed control for complex III activity was established, monitoring the reduction of oxidized cytochrome *c* over time (Fig. 5A) and validated with inhibition by antimycin A at 90 min (Fig. 5B). Flavins, nicotinamide reducing equivalents and Co-Q_{10} did not affect complex III activity (Fig. 5C). Moreover, MPP+ had no effect on complex III activity (Fig. 5D).

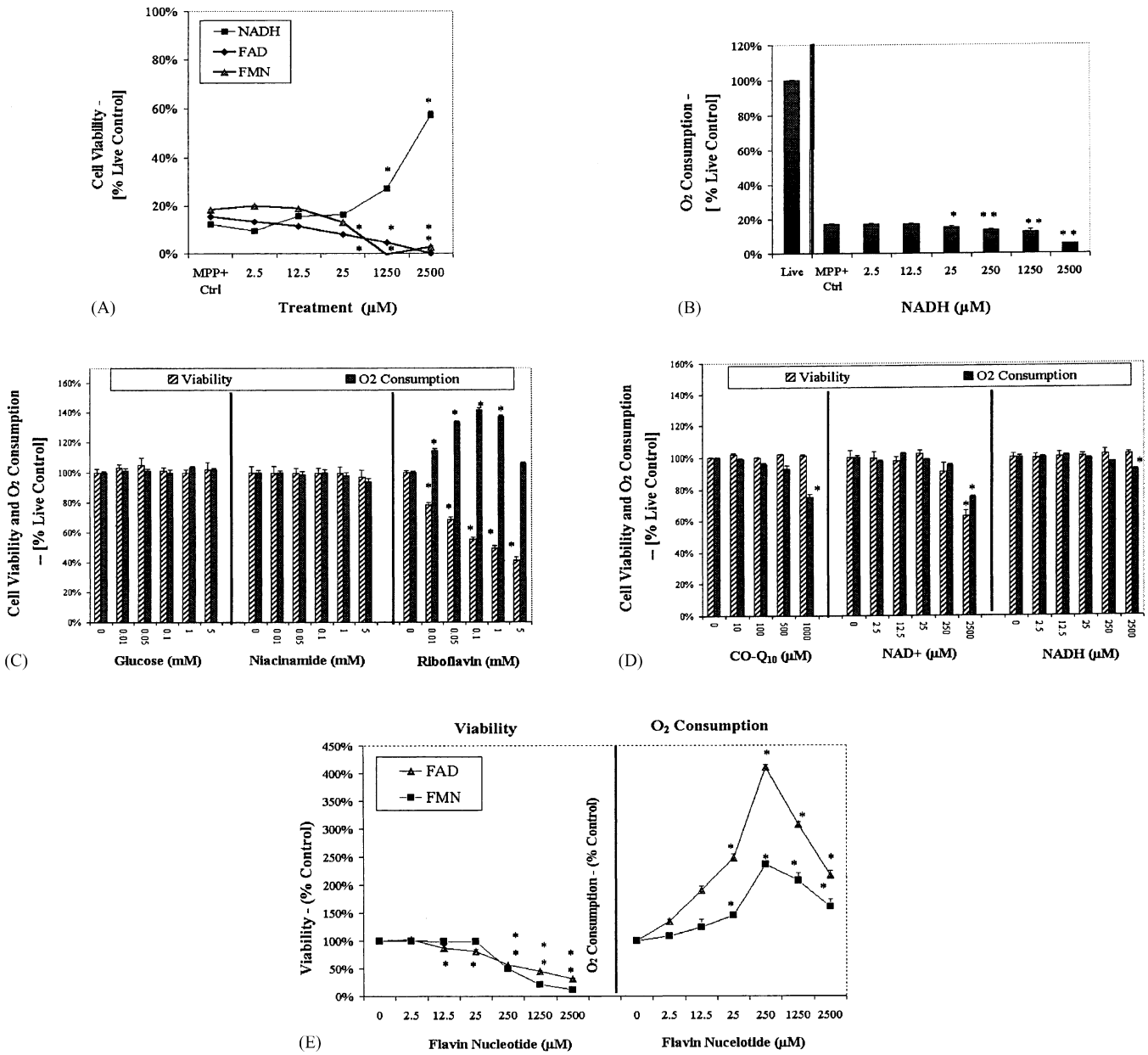

Fig. 2. (A) The cytoprotective effects of FAD, FMN and NADH on toxicity of MPP+ (500 μM) in N-2A cells. The data represent cell viability relative to live controls and are expressed as the mean ± SEM (N = 4). The significance of difference from the MPP+ treated controls were determined by a one-way ANOVA, followed by a Tukey mean comparison post hoc test, $^{*}P < 0.001$. (B) The effect of NADH on mitochondrial O_2 consumption during cytoprotection against MPP+ (500 μM) toxicity. The data represent O_2 consumption as percent of live controls and are expressed as the mean ± SEM (N = 4). The significance of difference from the MPP+ treated controls were determined by a one-way ANOVA, followed by a Tukey mean comparison post hoc test, $^{*}P < 0.001$. (C) Baseline effects of riboflavin, niacinamide and glucose on cell viability and whole cell O_2 consumption (in cells not treated with MPP+). The data represent viability and O_2 consumption as percent live controls and are expressed as the mean ± SEM (N = 4). The significance of difference from the controls were determined by a one-way ANOVA, followed by a Tukey mean comparison post hoc test, $^{*}P < 0.001$. (D) Baseline effects of Co-Q_{10}, NAD+ and NADH on cell viability and whole cell O_2 consumption (in cells not treated with MPP+). The data represent viability and O_2 consumption as percent live controls and are expressed as the mean ± SEM (N = 4). The significance of difference from the controls were determined by a one-way ANOVA, followed by a Tukey mean comparison post hoc test, $^{*}P < 0.001$. (E) Baseline effects of FAD and FMN on cell viability and whole cell O_2 consumption (in cells not treated with MPP+). The data represent viability and O_2 consumption as percent live controls and are expressed as the mean ± SEM (N = 4). The significance of difference from the live untreated controls were determined by a one-way ANOVA, followed by a Tukey mean comparison post hoc test, $^{*}P < 0.001$.

3.7. Complex IV

Up to this point the effects of MPP+ on complexes I–III, do not appear to correspond to the loss of mitochondrial O_2 consumption in whole cells. A complex IV inhibitor control was established by measuring the oxidation of reduced cytochrome *c* and inhibition by sodium azide at 60 min (Fig. 6A). A timed control for complex IV (Fig. 6B, left panel) was run in parallel with various concentrations of MPP+ (Fig. 6B, right panel). The data demonstrate

dose-dependent inhibition by MPP+ at 20, 55 and 75 min. Because of the high cell density required to assess ETC activities in isolated mitochondria over short time periods, the effects of MPP+ were also examined using a dilute concentration of mitochondrial isolate to represent activity in whole cells. Figure 6C displays a timed control for complex IV (left panel) run parallel to samples with various concentrations of MPP+ (right panel). The data demonstrate dose-dependent inhibition at 140, 240 and 300 min. These data clearly indicate that up to the first 140 min, in whole cells, extensive inhibition of complex IV may be a primary target of MPP+ and contribute to the loss of O_2 consumption by mitochondria.

3.8. Adverse effects of aerobic environment and metabolism

Neuroblastoma cells are analogous to cancer cells, with respect to an anomaly in anaerobic metabolism. The following data indicate that these cells prefer the lack of

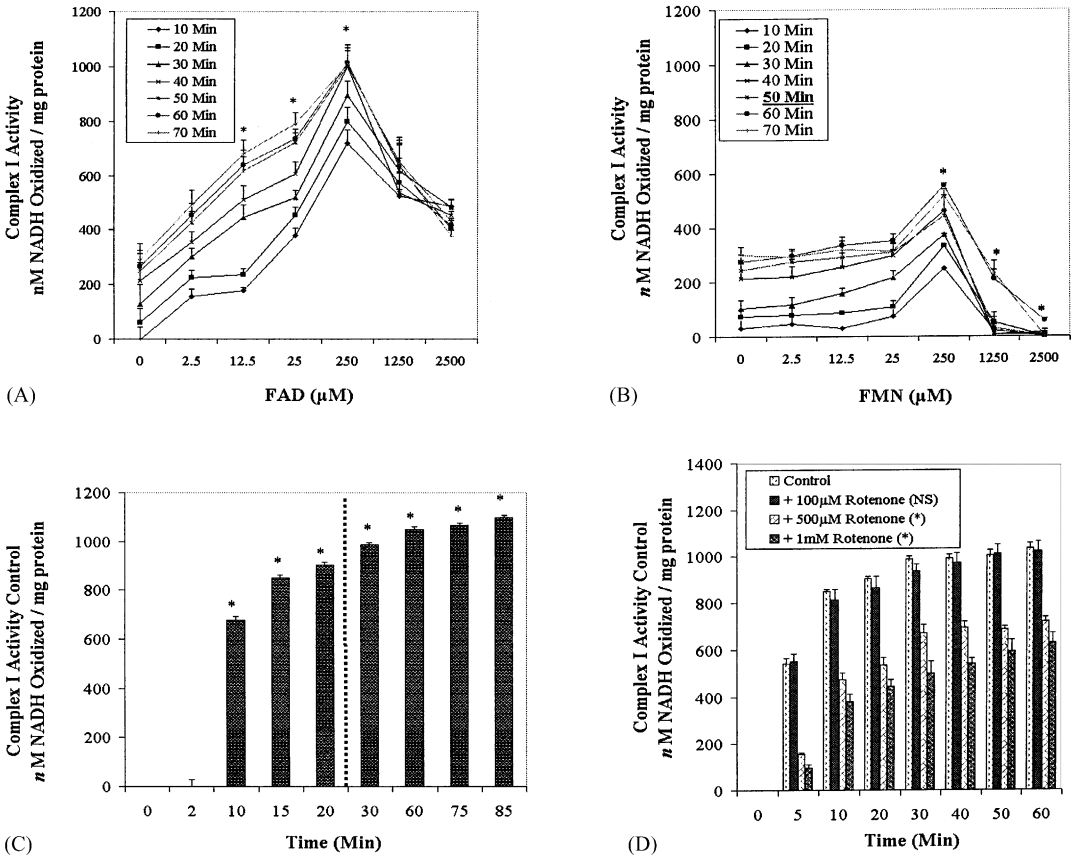

Fig. 3. (A) The effects of FAD on complex I activity in isolated mitochondria over time (0–70 min). The data represent enzyme velocity (nM NADH oxidized/mg protein) and are expressed as the mean ± SEM (N = 4). The significance of difference from the controls were determined by a one-way ANOVA, followed by a Tukey mean comparison post hoc test, $^{*}P < 0.001$ at 50 min. (B) The effect of FMN on complex I activity in isolated mitochondria over time (0–70 min). The data represent enzyme velocity (nM NADH oxidized/mg protein) and are expressed as the mean ± SEM (N = 4). The significance of difference from the controls were determined by a one-way ANOVA, followed by a Tukey mean comparison post hoc test, $^{*}P < 0.001$ at 50 min. (C) Complex I activity controls in isolated mitochondria over time (0–85 min). The data represent enzyme velocity (nM NADH oxidized/mg protein) and are expressed as the mean ± SEM (N = 4). The significance of difference from the controls (T_0) were determined by a one-way ANOVA, followed by a Tukey mean comparison post hoc test, $^{*}P < 0.001$. (D) Complex I activity in isolated mitochondria with variation in rotenone (100 μM–1 mM) over time (0–60 min). The data represent enzyme velocity (nM NADH oxidized/mg protein) and are expressed as the mean ± SEM (N = 4). The significance of difference from the control was determined by a two-way ANOVA, $^{*}P < 0.001$. (E) The effect of MPP+ on complex I activity in isolated mitochondria over time (10, 20, 30 min). The data represent enzyme velocity (nM NADH oxidized/mg protein) and are expressed as the mean ± SEM (N = 4). The significance of difference from the control was determined by a one-way ANOVA, followed by a Tukey mean comparison post hoc test, $^{*}P < 0.001$ at 30 min. (F) The effect of MPP+ (1 mM) (right panel) on NADH substrate driven complex I activity in isolated mitochondria over time (0–35 min) vs. untreated controls treated with PBS (left panel). The data represent enzyme velocity (nM NADH oxidized/mg protein) and are expressed as the mean ± SEM (N = 4). The significance of difference from the control was determined by a two-way ANOVA, $^{*}P < 0.001$ at 30 min. (G) The effects of Co-Q_{10} on MPP+ (1 mM) complex I inhibition in isolated mitochondria over time (0–35 min). The left panel displays effects of Co-Q_{10} (PBS control) and the right panel displays activity in the presence of Co-Q_{10} and MPP+ (1 mM). The data represent enzyme velocity (nM NADH oxidized/mg protein) and are expressed as the mean ± SEM (N = 4). The significance of difference from the controls was determined by a one-way ANOVA, followed by a Tukey mean comparison post hoc test at 30 min. There were no significant differences found. (H) The kinetic inhibition of MPP+ (1 mM) on complex I activity in the presence of various concentrations of FAD, FMN and NADH at 30 min. The data represent enzyme velocity (nM NADH oxidized/mg protein) ± MPP+ and are expressed as the mean ± SEM (N = 4).

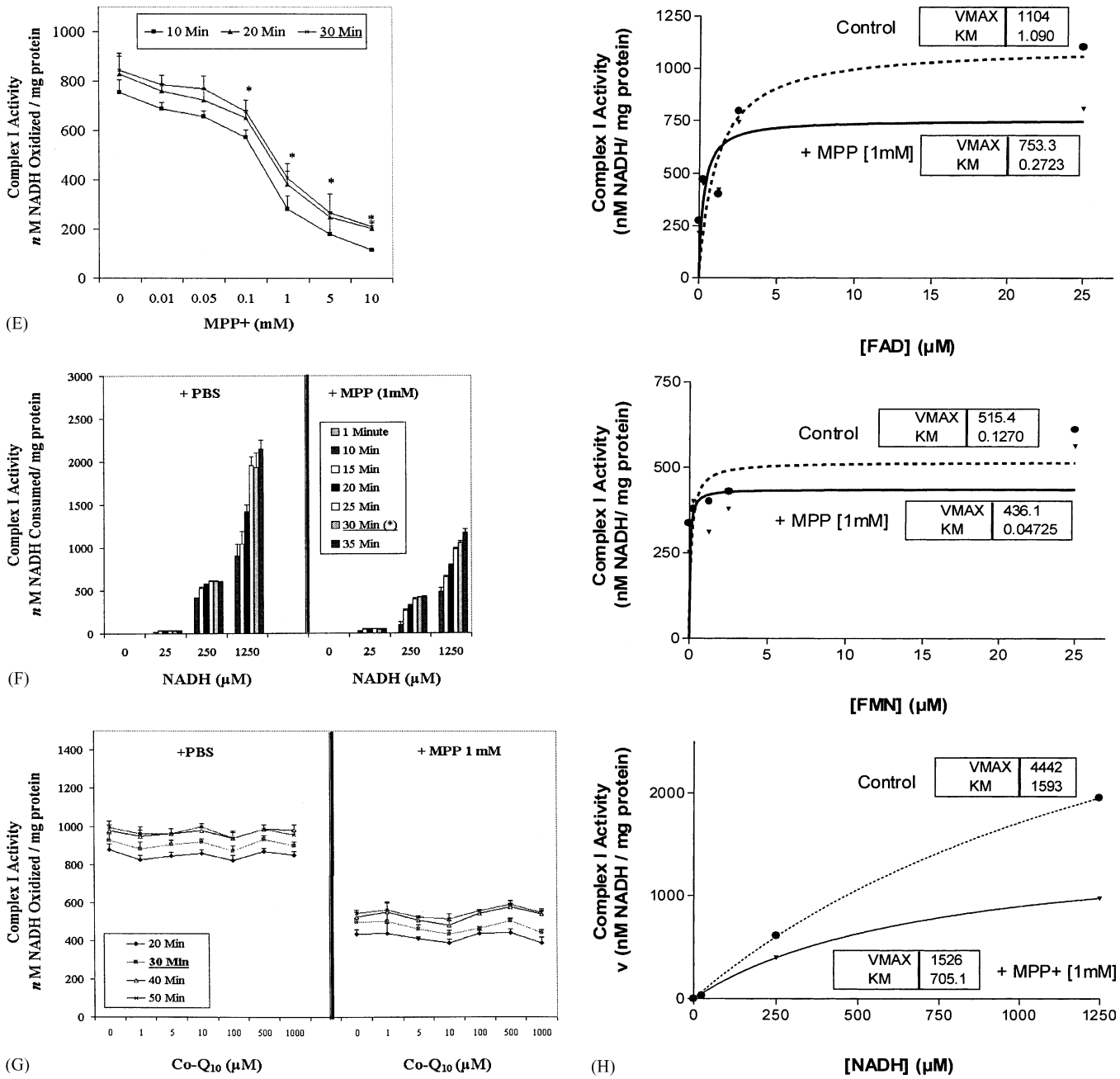

Fig. 3. (*Continued*).

O_2 or mitochondrial toxins when enough glucose is available. In contrast, creating an aerobic environment or enhancing aerobic function may be lethal. Previously, in Fig. 1B, we demonstrate that MPP+ induced accelerated utilization of glucose indicative of active glycolysis. Figure 7A corroborates that neuroblastoma cells readily survive and exhibit rapid use of glucose under conditions of dissolved O_2 deprivation (sodium dithionate), additional dissolved CO_2 (carbonated water), or in a closed chamber held at 30% CO_2/16% O_2 for 24 hr. All three conditions, and exposure to MPP+ created an anaerobic environment and enhanced use of glucose through active glycolysis. Toxicity (T) was not evident unless glucose was depleted from the medium. In contrast, Fig. 7A demonstrates that riboflavin, which increases mitochondrial O_2 consumption and aerobic respiration, attenuates cellular use of glucose, leading to cell death by metabolic inactivation or inability to utilize glucose. Similarly, creating an aerobic environment appears to be lethal. Figure 7B demonstrates that increasing aerobic conditions through raising ambient O_2 or the ratio of O_2/CO_2 is also toxic. The cells were placed in the incubator at standard conditions (5% CO_2/19.8% O_2) for 24 hr. The cell samples were then taken out of the incubator and exposed to regular air atmosphere (0.05% CO_2/20.5% O_2) at 37°. Air gas ratios were determined by a digital Bacharach—Model 2835 Analyzer. Oxygen saturation (dissolved O_2) within the

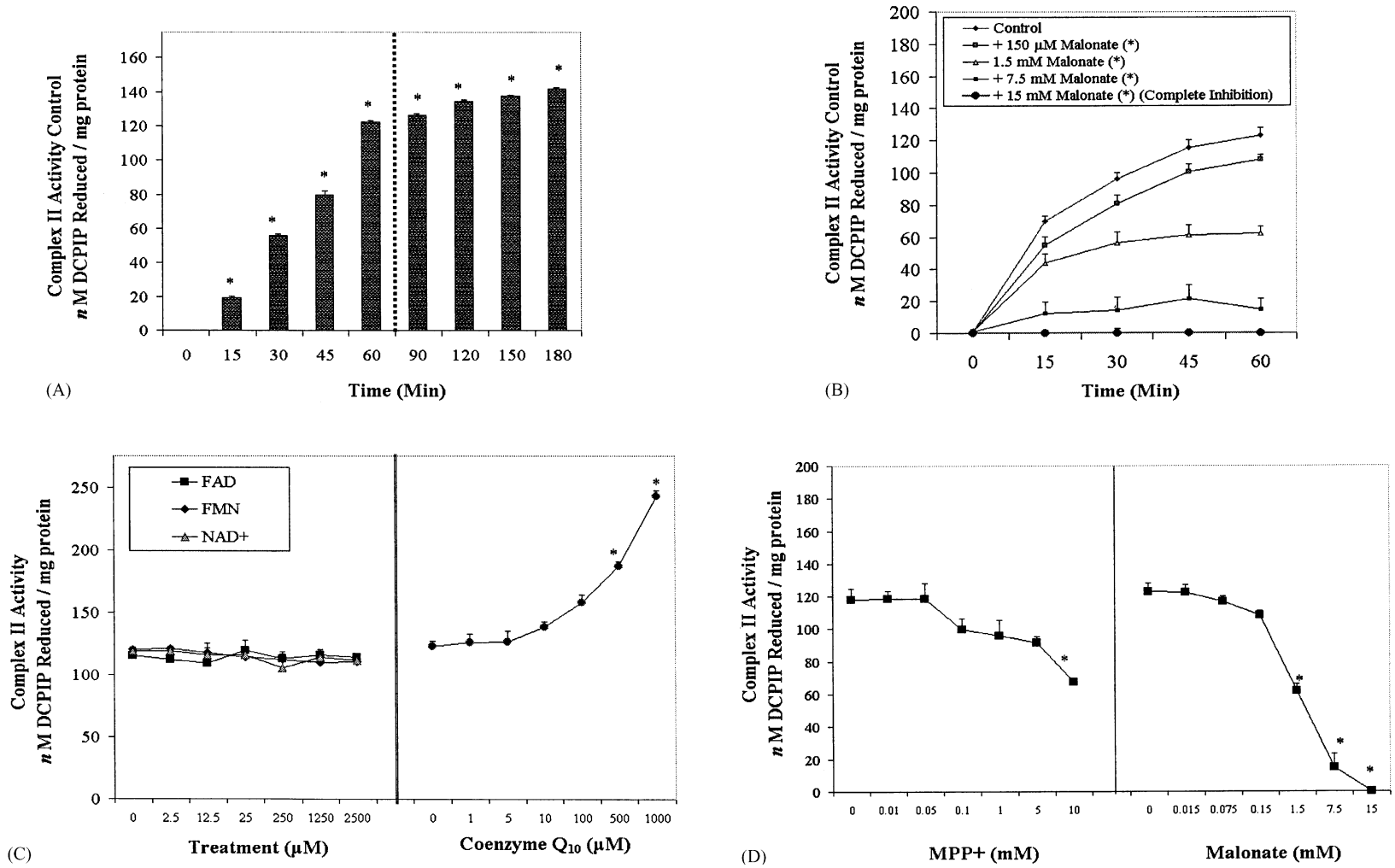

Fig. 4. (A) Complex II activity in isolated mitochondria measured over time (0–180 min). The data represent enzyme velocity (nM DCPIP reduced/mg protein) and are expressed as the mean ± SEM (N = 4). The significance of difference from the control (T_0) was determined by a one-way ANOVA, followed by a Tukey mean comparison post hoc test, $^*P < 0.001$. (B) Complex II activity controls in isolated mitochondria + variation in malonate (150 µM–15 mM) over 0–60 min. The data represent enzyme velocity (nM DCPIP reduced/mg protein) and are expressed as the mean ± SEM (N = 4). The significance of difference from the control was determined by a two-way ANOVA, $^*P < 0.001$. (C) The effects of FAD, FMN, NAD+ and Co-Q_{10} on complex II activity in isolated mitochondria at 60 min. The data represent enzyme velocity (nM DCPIP reduced/mg protein) and are expressed as the mean ± SEM (N = 4). The significance of difference from the controls were determined by a one-way ANOVA, followed by a Tukey mean comparison post hoc test, $^*P < 0.001$. (D) The effects of MPP+ and malonate on complex II activity in isolated mitochondria at 60 min. The data represent enzyme velocity (nM DCPIP reduced/mg protein) and are expressed as the mean ± SEM (N = 4). The significance of difference from the controls were determined by a one-way ANOVA, followed by a Tukey mean comparison post hoc test, $^*P < 0.001$.

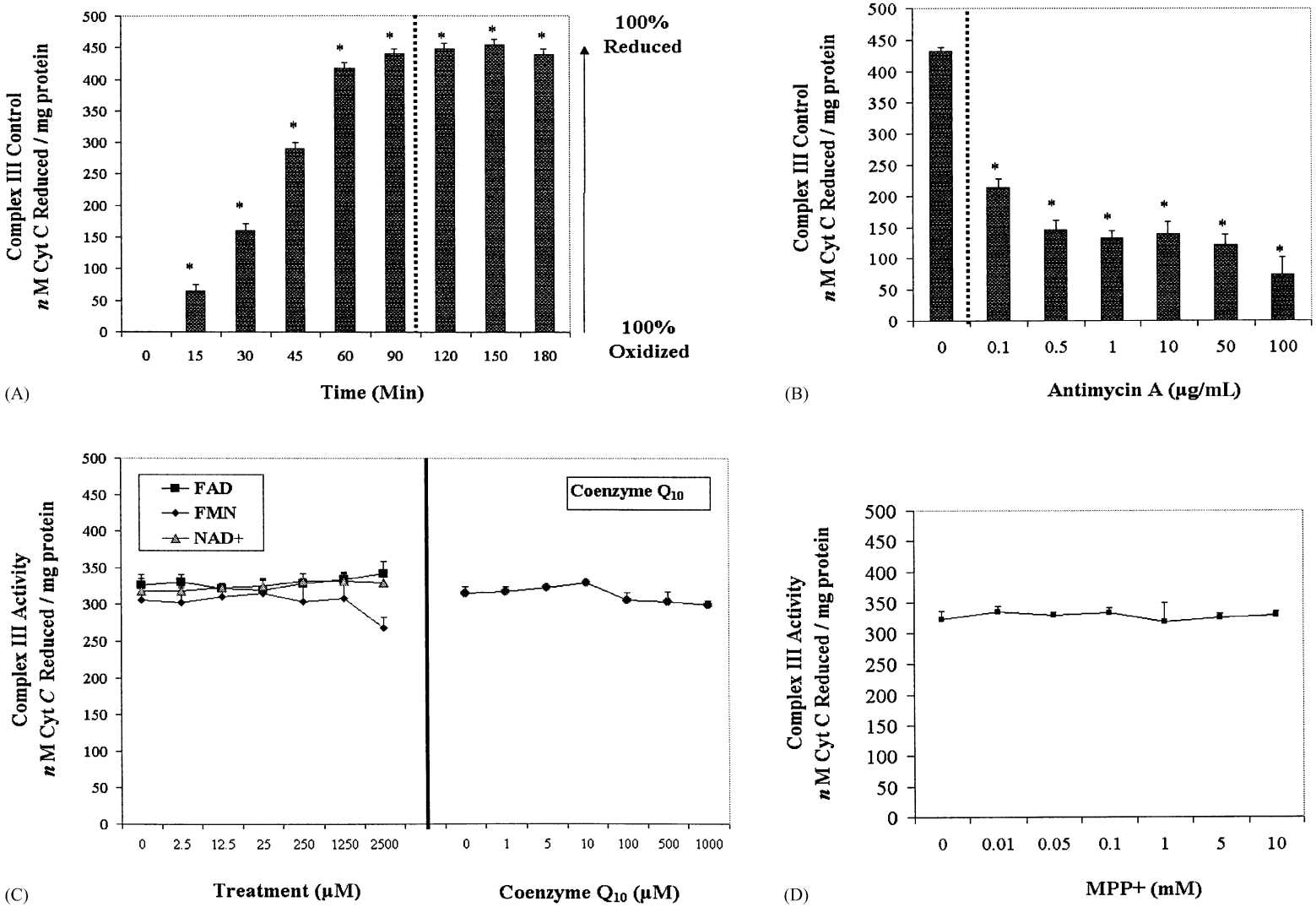

Fig. 5. (A) Complex III activity in isolated mitochondria measured over time (0–180 min). The data represent enzyme velocity (nM Cyt *c* reduced/mg protein) and are expressed as the mean ± SEM (N = 4). Reduced Cyt *c* was established with an ascorbic acid control, and at 90 min 100% of the oxidized form of Cyt *c* was reduced. The significance of difference from the control (T_0) was determined by a one-way ANOVA, followed by a Tukey mean comparison post hoc test, $^{*}P < 0.001$. (B) Complex III activity in the presence of varying concentration of antimycin A at 90 min. The data represent enzyme velocity (nM Cyt *c* reduced/mg protein) and are expressed as the mean ± SEM (N = 4). The significance of difference from the controls were determined by a one-way ANOVA, followed by a Tukey mean comparison post hoc test, $^{*}P < 0.001$. (C) The effects of FAD, FMN, NAD+ and Co-Q_{10} on complex III activity in isolated mitochondria at 45 min. Potential positive effects on enzyme velocity tests were acquired at 45 min, prior to full reduction, which occurred at 90 min. The data represent enzyme velocity (nM Cyt *c* reduced/mg protein) and are expressed as the mean ± SEM (N = 4). The significance of difference from the controls was determined by a one-way ANOVA, followed by a Tukey mean comparison post hoc test. There were no significant differences determined. (D) The effect of MPP+ on complex III activity in isolated mitochondria at 45 Min. The data represent enzyme velocity (nM Cyt *c* reduced/mg protein) and are expressed as the mean ± SEM (N = 4). The significance of difference from the controls was determined by a one-way ANOVA, followed by a Tukey mean comparison post hoc test. There were no significant differences determined.

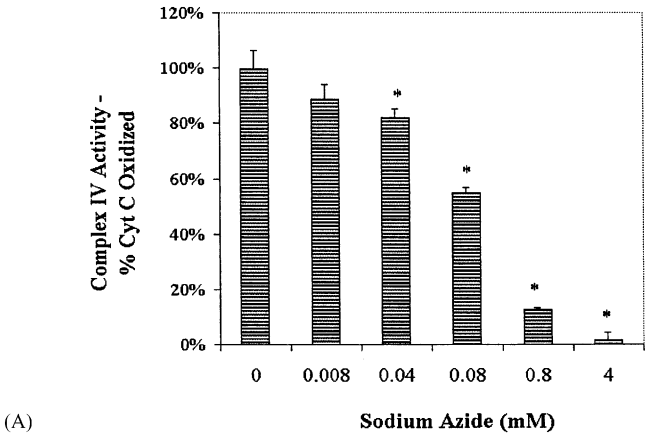

(A)

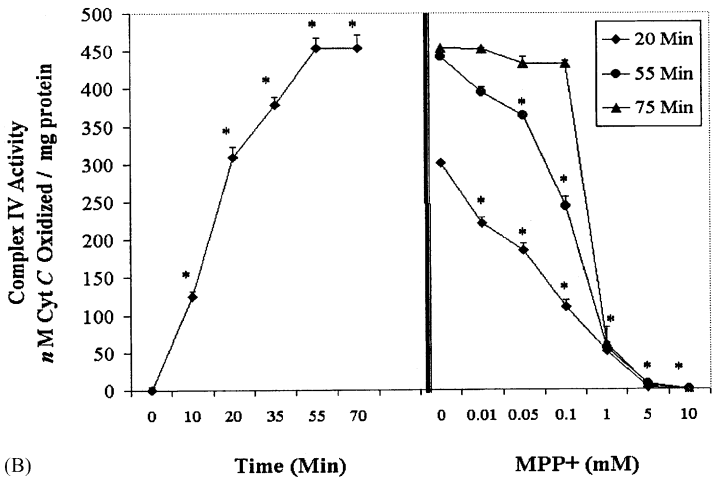

(B)

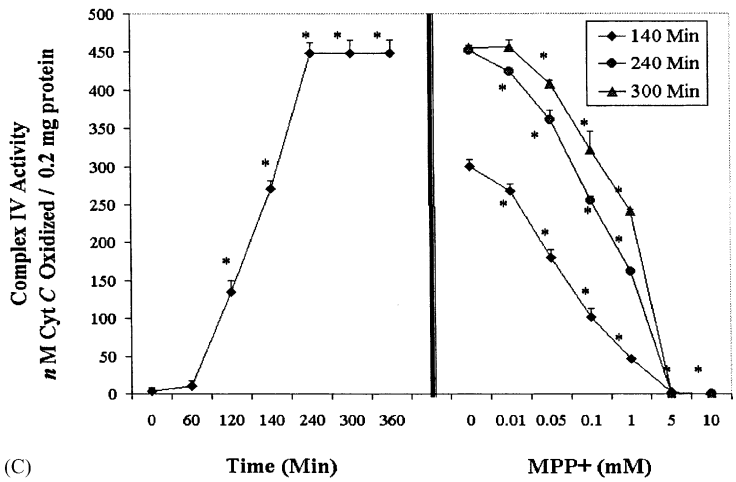

(C)

Fig. 6. (A) Complex IV activity in isolated mitochondria in the presence of varying concentration of Na^{2+} azide at 60 min. The data represent enzyme velocity (percent Cyt *c* oxidized) and are expressed as the mean ± SEM (N = 4). The significance of difference from controls were determined by a one-way ANOVA, followed by a Tukey mean comparison post hoc test, $^{*}P < 0.001$. (B) Complex IV activity in isolated mitochondria was examined over time (0–70 min) (left panel). The data represent enzyme velocity (nM Cyt *c* oxidized/mg protein) and are expressed as the mean ± SEM (N = 4). Reduced cytochrome *c* was established with ascorbic acid, relative to the oxidized form of Cyt *c*. At 55 min 100% of the reduced Cyt *c* was oxidized. The effects of MPP+ on complex IV activity were determined at 20, 55 and 75 min (right panel). The data represent enzyme velocity (nM Cyt *c* oxidized/mg protein) and are expressed as the mean ± SEM (N = 4). The significance of difference from the controls were determined by a one-way ANOVA, followed by a Tukey mean comparison post hoc test, $^{*}P < 0.001$. (C) Complex IV activity controls in diluted isolated mitochondria preparation (50 μg/mL protein) were examined over time (0–360 min) (left panel). The data represent enzyme velocity (nM Cyt *c* oxidized/0.2 mg protein) and are expressed as the mean ± SEM (N = 4). The effects of MPP+ on complex IV activity were determined at 140, 240 and 300 min (right panel). The data represent enzyme velocity (nM Cyt *c* oxidized/0.2 mg protein) and are expressed as the mean ± SEM (N = 4). The significance of difference from controls were determined by a one-way ANOVA, followed by a Tukey mean comparison post hoc test, $^{*}P < 0.001$.

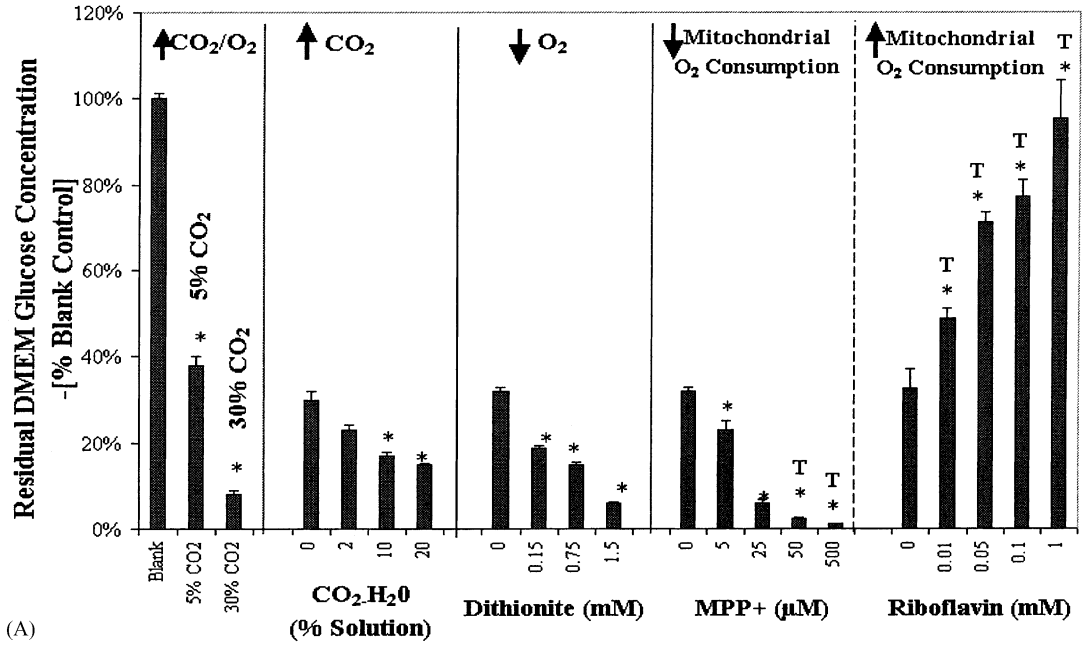

(A)

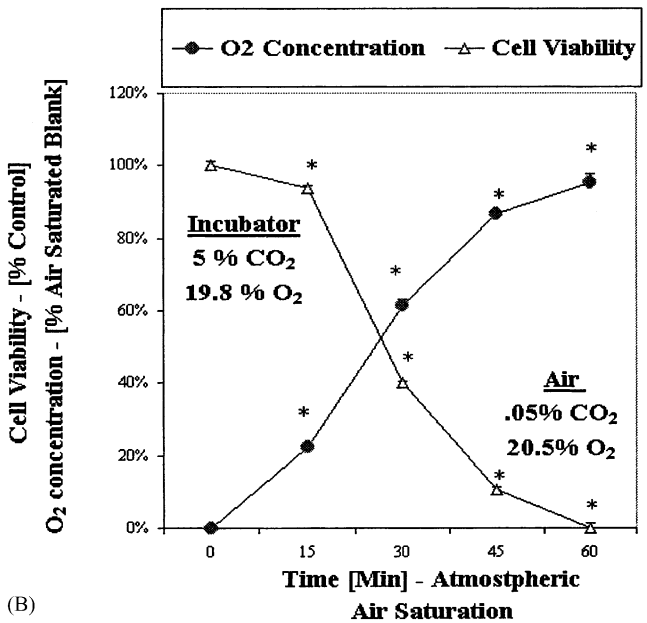

(B)

Fig. 7. (A) The effect of 30% CO_2, carbonated water (CO_2 H_2O), Na^{2+} dithionite, MPP+ and riboflavin on glucose use by N-2A cells. The data represent DMEM glucose concentration relative to the control blank and are expressed as the mean ± SEM (N = 4). The significance of difference from the controls (T_0) were determined by a one-way ANOVA, followed by a Tukey mean comparison post hoc test, $^*P < 0.001$. Loss of cell viability was also monitored. "T" represents toxicity evident for each group at 24 hr. (B) The effect of air saturation on N-2A cell death at 37°. The data represent viability as percent live control, and dissolved O_2 concentration in the medium as percent of saturated control blank as determined by Clark electrode. The CO_2/O_2 concentration of the air inside the incubator was (5.0% CO_2/19.8% O_2) and atmosphere outside the chamber was (0.05% CO_2/20.5% O_2). The data are expressed as the mean ± SEM (N = 4). The significance of difference from the controls (T_0) were determined by a one-way ANOVA, followed by a Tukey mean comparison post hoc test, $^*P < 0.001$.

medium was monitored with a Clark electrode. After 60 min in atmosphere, the cells were 100% dead, indicating a metabolic requirement for CO_2.

In summary, these findings indicate the MPP+ exerts predominant inhibitory effects on complexes 1–IV. In addition, riboflavin derivatives control the rate of mitochondrial respiration and complex I activity. This study also demonstrates an anomaly of neuroblastoma with regards to anaerobic preference and adversity to aerobic conditions.

4. Discussion

Aerobic glucose oxidation through mitochondrial OXPHOS requires the channeling of reducing equivalents to the ETC for synthesis of ATP. The ETC consists of five mitochondrial enzyme complexes located on the inner mitochondrial membrane. Complexes I–IV transfer protons through redox reactions with functional requirements including supply of nicotinamide (NADH), flavins (FMN, FAD), Co-Q_{10}, non-heme-iron copper proteins and cytochromes [28]. The results in this study indicate that MPP+ exerts detrimental effects on mitochondrial function through simultaneous inhibition of complexes I and IV. Moreover, complex IV inhibition most paralleled the loss of MOC in whole cells, and explained the lack of cytoprotection during potentiation of complexes I–II activity with flavins and Co-Q_{10}.

Previous research is consistent in describing a dose-dependent decline in O_2 consumption with exposure to MPP+ [29,30], one that is consistent with metabolic aberrations occurring in PD patients [1,31]. Further, the literature is consistent in describing complex I as a target of MPP+, or structural analogues such as 1,2,3,4-tetrahydroisoquinolines, isoquinoline derivates and *N*-methylated beta-carbolinium in a variety of tissue, primary cells and immortal cell lines [15,16,30,32,33]. On the other hand, results regarding a role for MPP+ on complex II have been inconsistent. For example, while most studies have confirmed the effects of MPP+ on complex II in insolated mitochondria are negligible [15,34,35], others reported complex II inhibition by MPP+ occurs at concentrations approximately 7-fold higher [36]. The findings in this study are consistent with the majority of previous research regarding specific effects of MPP+ on O_2 consumption, loss of ATP and the reduction of complex I, with slight effects on complex II activity [15,19,37].

The findings in this study are also comparable in terms of concentration of MPP+ required to inhibit complex I. In other studies, 10 mM MPP+ in beef heart mitochondria caused a 52% decrease in complex I activity after 1 hr [14]. In another study, 10 mM MPP+ caused about a 75% inhibition after 30 min [15]. However, it is important to note that in this study, complex I activity was extremely rapid, relative to complexes II–IV. This may be due to non-specific NADH dehydrogenases which may have influenced quantification of baseline enzyme activity, possibly leading to the underestimation of quantified effects on complex I. Despite this potential interference, the effects of MPP+ on NADH dehydrogenase in complex I did not appear to account for impairment of mitochondrial O_2 consumption in whole cells. On the other hand, the data acquired on MPP+ inhibition of complex IV closely paralleled loss of O_2 consumption in whole cells. Moreover, complex IV is responsible for controlling mitochondrial respiration by converting O_2 into H_2O, a seemingly plausible target. Although our findings are in contrast to McNaught *et al*. [16], they are similar to Desai *et al*. [38], who also reported effects of MPP+ on both complexes I (85% reduction) and IV (75% reduction) in primary neurons derived from mouse brain. Desai *et al.*, also reports recovery, which we found to be the case over time, in particular in complex I activity. While the data in this study reflect the effects of MPP+ at 30 min on complex I, at 60 min it was interesting to note that even 10 mM of MPP+ had negligible inhibitory effects.

The results from this study, indicate a predominant role of MPP+ on complex IV. While there has been little focus on the study of complex IV in the pathogenesis of PD, idiopathic PD patients consistently exhibit combined complexes I–IV abnormalities in peripheral tissue [39–43]. And, similar to the findings in this study, extent of complex IV impairment in the mitochondria of PD patients, are reportedly greater than those observed for complex I (68 and 26% reduction, respectively) [39]. Moreover, *in vivo* studies examining the effects of MPTP in non-human primates indicate selective targeting toward complex IV. MPTP administration to the cynomolgus monkey is associated with complex IV dysfunction and selective damage to dopaminergic cerebral cortex and hippocampus nerve terminals [44]. Similarly, Pastoris *et al*. [45], found administration of MPTP in monkeys to be associated with skeletal mitochondria deficiencies, primarily involving complex IV, rather than complex I. And, in human idiopathic PD, altered mitochondrial respiratory chain function in skeletal muscle and platelets also reveal anomalies consistent with a dual complexes I–IV deficiency [39–42].

It is important to note the modifications made from existing protocols in this study to measure complex IV. While measuring complexes I and II were straightforward, complex IV activity was not detected using existing protocols in method validation controls. In addition, we noticed that several other protocols did not apply mitochondrial inhibitors during cytochrome oxidase (IV) testing. We hypothesized that non-response was due to the fact that complex IV activity cannot be quantified due to the canceling out by complex III. Cytochrome *c* reductase and cytochrome *c* oxidase are equal and opposite reactions, occurring in tandem. Therefore, the method design involved the hampering of any redox activity occurring through complex II with malonate and III with antimycin. Interesting, this method design was very sensitive for the detection of complex IV activity leading to complete oxidation of reduced cytochrome, which was validated by inhibition with sodium azide. It was also interesting to note that our results corroborate an increase of MTT dye cleavage, during cytoprotection against MPP+ with glucose, despite loss of mitochondrial function (data not shown). However, the increase of cleavage did not correspond to an increase of complex I activity. The explanation for this was elucidated by our finding that the majority of MTT cleavage (>90%), was performed by the dehydrogenases within the cytosolic compartment, rather than

mitochondrial NADH dehydrogenase. These findings suggest that MTT can detect viability achieved through anaerobic energy metabolism, and therefore it is a valid toxicity assay to study effects of mitochondrial toxins *in vitro*.

The impairment of mitochondrial function in neurons, can lead to energy failure due to loss of ATP produced through OXPHOS, rending a vulnerability to degenerate. It is not known to what extent flavin and nicotinamide reducing equivalents can overcome mitochondrial dysfunction. One of the unexpected findings in this study was the fact that flavins, and not the supply of glucose, are controlling aerobic cellular respiration rate in the whole cells. The findings in this study also demonstrate that OXPHOS is not regulated by additional supply of nicotinamides or Co-Q_{10}. On the other hand, riboflavin and flavin nucleotides were powerful regulators of both complex I and cell respiration. These findings demonstrate a clear and important role for riboflavin in aerobic energy metabolism. These data also corroborate circumscribing reports demonstrating riboflavin deficiencies to be intricately associated with mitochondrial dysfunction, often characterized by loss of β-oxidation of fatty acids and acyl-CoA dehydrogenase [46]. Therapeutic administration of riboflavin can reverse or attenuate clinical and morphological symptoms of complex I disorders including exercise intolerance and myopathy [47–49]. Elevation of blood lactate associated with riboflavin deficiencies, are a clear indication of its global effects on mitochondrial respiration within the human body [49]. Interestingly, with significant evidence suggesting riboflavin could benefit complex I disorders, this had not yet been investigated for treatment of PD. And, previous understanding of complex I dysfunction in PD, would indicate therapeutic gain by riboflavin that could not be achieved by Co-Q_{10}. However, the findings in this study also demonstrate that complex IV is a predominant target of MPP+ in OXPHOS dysfunction. Therefore, it is uncertain if therapeutic administration of riboflavin would be effective. Future research will be required.

While riboflavin exerts pronounced effects on aerobic capacity, these data support a primary role for nicotinamide in propelling anaerobic metabolism. In neuroblastoma, the anaerobic glycolytic pathway predominates and in the absence of mitochondrial function, pyruvate is metabolized to lactic acid with the oxidation of NADH to NAD+ by lactic acid dehydrogenase. The NAD+ is required to propel ATP production through phosphoglycerate kinase and pyruvate kinase [50]. Although NADH+ plays a critical role in aerobic metabolism, in neuroblastoma, cytoprotection was observed through anaerobic potentiation. The current study demonstrates that cytoprotection can be achieved through propelling the anaerobic survival response. However, it is important to note that immortal cell lines have an aberrant metabolism, one that is divergent from normal oxidative processes typical to eukaryotic cells. Neuroblastoma are characteristic in many ways to cancer cells, which display the Warburg effect, a high

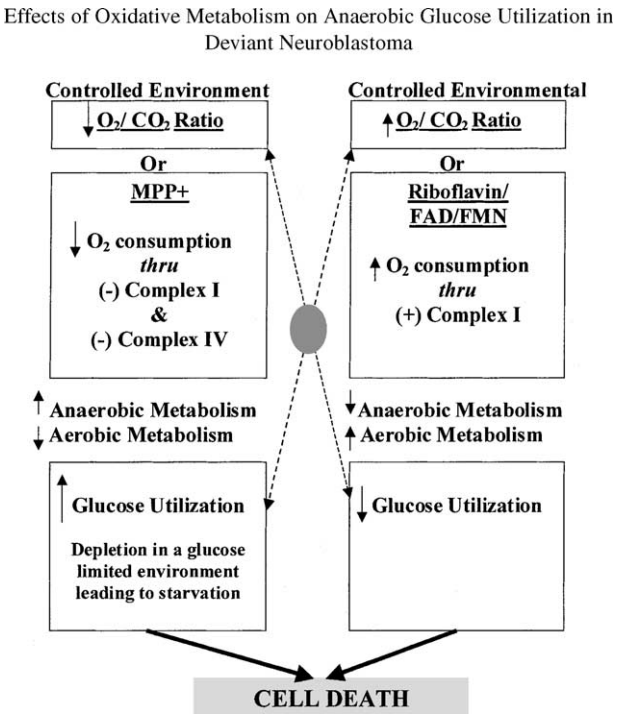

Fig. 8. Anaerobic preference and adverse effects of aerobic conditions on neuroblastoma indicating two modes of cell death. The following schematic is a brief description describing the inverse relationship between a reduction in MOC, and anaerobic conditions that foster enhanced glycolytic activity, leading to glucose depletion and starvation. Conversely, aerobic conditions or enhanced MOC appears to disrupt glycolysis or glucose utilization through an unknown mechanism. In summary, neuroblastoma cells have ability to thrive under completely anaerobic conditions, given that glucose supply is sustained.

glycolytic activity occurring in the absence or presence of oxygen, rapid cell proliferation and an accumulation of lactic acid [51–53]. The results from this study, corroborate existing knowledge that these cells inherently prefer anaerobic conditions, however, it is novel to demonstrate that the cells appear to react adversely to aerobic conditions.

Figure 8 is an overview of this finding. Briefly, increasing the ambient O_2 concentration and reducing CO_2 appeared to be a lethal combination. In addition, there appears to be an inverse relationship between MPP+ and riboflavin. MPP+ inhibits MOC, complexes I and IV, and riboflavin increases complex I and MOC. The loss of OXPHOS is related to rapid glucose utilization through glycolysis, where the increase in OXPHOS reduces cellular ability to utilize glucose. Similarly, O_2 deprivation accelerates glucose utilization, where increasing O_2 prevents the use of glucose. It is interesting to note, that the described inverse relationship demonstrated in this study is similar to many cancer reports. *In vivo* studies indicate that deprivation of O_2 through hypoxia in mammary carcinoma is associated with increased glucose used through glycolysis [54] and aggressive malignancy [55]. On the other hand, the elevation in O_2 as an adjunct cancer treatment involving the use of carbogen (95% O_2/5% CO_2) might be related to the current findings. Carbogen is effective in improving

radiotherapeutic response to transplanted rat prolactinomas [56]. In a very similar fashion, hyperbaric O_2 treatment has been helpful to arrest the growth of tumors resistant to chemotherapy, such as hypoxic epithelial ovarian cancer, and can potentiate the toxic effects of chemotherapy drugs such as cisplatin [57].

While the use of immortal cell lines may be limited, valuable information can be obtained on anaerobic survival against mitochondrial toxins. Anaerobic metabolism occurs in the human brain and evidence suggests that CNS neurons have abundant anaerobic glycolytic activity [58]. Introduction of mitochondrial toxins such as MPP+ or beta-carbolinium *in vivo* into the striatum of freely moving rats, results in accumulation of lactic acid, indicating anaerobic compensatory survival response [59]. *In vivo*, central nervous system neurons can rapidly shift toward a high requirement for anaerobic glycolysis under conditions such as electrical stimulation [60] ischemic head injury [61] physiological restraint, stress [62] and mitochondrial disorders [63]. These findings indicate an important requirement for CNS neurons to sustain energy driven processes through anaerobic glycolysis, in particular during diseases such as PD that involve mitochondrial abnormalities.

The data in this investigation and our previous studies corroborate that the source of ATP produced during the cytoprotection of glucose and other glycolytic intermediates against MPP+ toxicity in neuroblastoma [19,21,64] may be related to glycolytic abilities of the cells without the involvement of complex V of the ETC. This rationale is based on evidence that MOC is completely blocked (close to 0% of controls), during cytoprotection with glucose and glycolytic intermediates. The accumulation of lactic acid corresponds to rapid consumption of glucose through glycolysis, denoting anaerobic production of ATP through substrate level phosphorylation. Measurement of MOC, gives valuable information on the function of the mitochondrial ETC and capacity of ATP to be produced through complex V–OXPHOS. Oxygen is the final and terminal electron acceptor of the ETC. At complex IV, electrons are eventually accepted from reduced cytochrome *c* and transferred to O_2 to produce H_2O. A reduction in MOC, represents the failure of both electron transfers in the chain and proton translocation. For ATP to be produced by mitochondrial OXPHOS, a proton motive force must be established and this requires functional complexes I, III and IV. Electron transfer by complexes I, III, and IV, results in H^+ translocation from the mitochondrial matrix into the intermembrane space leading to proton gradient. This proton motive force is required to drive the oxidative production of ATP through F_1F_0 ATP synthase [65,66]. The subunit of F_0 in the membrane protein complex of ATPase, is a proton pore that is driven by H+ current. In order, for ATP to be produced through OXPHOS, a H+ gradient must be established to drive the synthesis of ATP by the mitochondria. When MPP+ is present, electron transfer and H+ transport through complexes I and IV are hampered, indirectly inhibiting ATP production through complex V. Future research will be required to assess the direct effects of MPP+ on complex V function. Since the effects of MPP+ on OXPHOS appear to be irreversible, anaerobic production of ATP becomes critical to sustain viable cell function.

In conclusion, the data presented in this study reveal dual targeting effects of MPP+ on complexes I and IV. Furthermore, these findings indicate stimulating effects of NADH, FAD, FMN, riboflavin and Co-Q_{10} on complex I and II activities and aerobic function, and NADH on anaerobic glycolysis.

Acknowledgments

The authors would like to acknowledge the support of the National Institutes of Health grant (RR03020) to this research investigation.

References

[1] Ebadi M, Govitrapong P, Sharma S, Muralikrishnan D, Shavali S, Pellett L, Schafer R, Albano C, Eken J. Ubiquinone (coenzyme q10) and mitochondria in oxidative stress of Parkinson's disease. Biol Signals Recept 2001;10:224–53.

[2] Betarbet R, Sherer TB, MacKenzie G, Garcia-Osuna M, Panov AV, Greenamyre JT. Chronic systemic pesticide exposure reproduces features of Parkinson's disease. Nat Neurosci 2000;3:1301–6.

[3] Blass JP. Glucose/mitochondria in neurological conditions. Int Rev Neurobiol 2002;51:325–76.

[4] van der Walt JM, Nicodemus KK, Martin ER, Scott WK, Nance MA, Watts RL, Hubble JP, Haines JL, Koller WC, Lyons K, Pahwa R, Stern MB, Colcher A, Hiner BC, Jankovic J, Ondo WG, Allen Jr FH, Goetz CG, Small GW, Mastaglia F, Stajich JM, McLaurin AC, Middleton LT, Scott BL, Schmechel DE, Pericak-Vance MA, Vance JM. Mitochondrial polymorphisms significantly reduce the risk of Parkinson disease. J Hum Genet 2003;72:804–11.

[5] Kosel S, Hofhaus G, Maassen A, Vieregge P, Graeber MB. The role of mitochondria in Parkinson's disease. Biol Chem 1999;380:865–70.

[6] Greenamyre JT, Sherer TB, Betarbet R, Panov AV. Complex I and Parkinson's disease. IUBMB Life 2001;52:135–41.

[7] Sherer TB, Betarbet R, Greenamyre JT. Environment, mitochondria, and Parkinson's disease. Neuroscientist 2002;8:192–7.

[8] Sherer TB, Betarbet R, Stout AK, Lund S, Baptista M, Panov AV, Cookson MR, Greenamyre JT. An *in vitro* model of Parkinson's disease: linking mitochondrial impairment to altered alpha-synuclein metabolism and oxidative damage. J Neurosci 2002;22:7006–15.

[9] Langston JW, Langston EB, Irwin I. MPTP-induced Parkinsonism in human and non-human primates—clinical and experimental aspects. Acta Neurol Scand Suppl 1984;100:49–54.

[10] Kotake Y. Tetrahydroisoquinoline derivatives as possible Parkinson's disease-inducing substances. Yakugaku Zasshi 2002;122:975–82.

[11] Naoi M, Maruyama W, Akao Y, Yi H. Dopamine-derived endogenous *N*-methyl-(*R*)-salsolinol: its role in Parkinson's disease. Neurotoxicol Teratol 2002;24:579–91.

[12] Maruyama W. Pathogenesis of idiopathic Parkinson's disease. Nippon Ronen Igakkai Zasshi 2001;38:494–7.

[13] Shen XM, Li H, Dryhurst G. Oxidative metabolites of 5-*S*-cysteinyldopamine inhibits the alpha-ketoglutarate dehydrogenase complex:

possible relevance to the pathogenesis of Parkinson's disease. J Neural Transm 2000;107:959–78.
[14] Cleeter MW, Cooper JM, Schapira AH. Irreversible inhibition of mitochondrial complex I by 1-methyl-4-phenylpyridinium: evidence for free radical involvement. J Neurochem 1992;58:786–9.
[15] Uzuki K, Mizuno Y, Yamauchi Y, Nagatsu T, Mitsuo Y. Selective inhibition of complex I by *N*-methylisoquinolinium ion and *N*-methyl-1,2,3,4-tetrahydroisoquinoline in isolated mitochondria prepared from mouse brain. J Neurol Sci 1992;109:219–23.
[16] McNaught KS, Thull U, Carrupt PA, Altomare C, Cellamare S, Carotti A, Testa B, Jenner P, Marsden CD. Inhibition of complex I by isoquinoline derivatives structurally related to 1-methyl-4-phenyl-1,2,3,6-tetrahydropyridine (MPTP). Biochem Pharmacol 1995;50: 1903–11.
[17] Muller T, Buttner T, Gholipour AF, Kuhn W. Coenzyme Q10 supplementation provides mild symptomatic benefit in patients with Parkinson's disease. Neurosci Lett 2003;341:201–4.
[18] Lenaz G, Parenti Castelli G, D'Aurelio M, Bovina C, Formiggini G, Marchetti M, Estornell E, Rauchova H. Coenzyme Q deficiency in mitochondria: kinetic saturation vs. physical saturation. Mol Aspects Med 1997;18:S25–31.
[19] Mazzio E, Soliman KF. D-(+)-Glucose rescue against 1-methyl-4-phenylpyridinium toxicity through anaerobic glycolysis in neuroblastoma cells. Brain Res 2003;962:48–60.
[20] Storch A, Kaftan A, Burkhardt K, Schwarz J. 1-Methyl-6,7-dihydroxy-1,2,3,4-tetrahydroisoquinoline (salsolinol) is toxic to dopaminergic neuroblastoma SH-SY5Y cells via impairment of cellular energy metabolism. Brain Res 2000;855:67–75.
[21] Mazzio E, Soliman KFA. Pyruvic acid cytoprotection against 1-methyl-4-phenylpyridinium, 6-hydroxydopamine and hydrogen peroxide toxicities. Neurosci Lett 2003;337:77–80.
[22] Notter MF, Irwin I, Langston JW, Gash DM. Neurotoxicity of MPTP and MPP+ *in vitro*: characterization using specific cell lines. Brain Res 1988;456:254–62.
[23] Evans SM, Casartelli A, Herreros E, Minnick DT, Day C, George E, Westmoreland C. Development of a high throughput *in vitro* toxicity screen predictive of high acute *in vivo* toxic potential. Toxicol in Vitro 2001;15:579–84.
[24] Naslund B, Arner P, Bolinder J, Hallander L, Lundin A. Glucose determination in samples taken by microdialysis by peroxidase-catalyzed luminal chemiluminescence. Anal Biochem 1991;192:237–42.
[25] Zhang J, Block ER, Patel JM. Down-regulation of mitochondrial cytochrome *c* oxidase in senescent porcine pulmonary artery endothelial cells. Mech Ageing Dev 2002;123:1363–74.
[26] Brusque AM, Borba Rosa R, Schuck PF, Dalcin KB, Ribeiro CA, Silva CG, Wannmacher CM, Dutra-Filho CS, Wyse AT, Briones P, Wajner M. Inhibition of the mitochondrial respiratory chain complex activities in rat cerebral cortex by methylmalonic acid. Neurochem Int 2002;40:593–601.
[27] Lowry OJ, Rosebrough NJ, Farr AL, Randall RJ. Protein measurement with Folin phenol reagent. J Biol Chem 1951;193:265–75.
[28] Greenamyre JT, MacKenzie G, Peng TI, Stephans SE. Mitochondrial dysfunction in Parkinson's disease. Biochem Soc Symp 1999;66: 85–97.
[29] Hasegawa E, Kang D, Sakamoto K, Mitsumoto A, Nagano T, Minakami S, Takeshige K. A dual effect of 1-methyl-4-phenylpyridinium (MPP+)-analogs on the respiratory chain of bovine heart mitochondria. Arch Biochem Biophys 1997;337:69–74.
[30] Conn KJ, Ullman MD, Eisenhauer PB, Fine RE, Wells JM. Decreased expression of the NADH: ubiquinone oxidoreductase (complex I) subunit 4 in 1-methyl-4-phenylpyridinium-treated human neuroblastoma SH-SY5Y cells. Neurosci Lett 2001;306:145–8.
[31] Di Monte DA. Mitochondrial DNA and Parkinson's disease. Neurology 1991;41:38–42.
[32] Bates TE, Heales SJ, Davies SE, Boakye P, Clark JB. Effects of 1-methyl-4-phenylpyridinium on isolated rat brain mitochondria: evidence for a primary involvement of energy depletion. J Neurochem 1994;63:640–8.
[33] Gonzalez-Polo RA, Soler G, Alonso JC, Rodriguez-Martin A, Fuentes JM. MPP (+) causes inhibition of cellular energy supply in cerebellar granule cells. Neurotoxicology 2003;24:219–25.
[34] Krueger MJ, Tan AK, Ackrell BA, Singer TP. Is complex II involved in the inhibition of mitochondrial respiration by *N*-methyl-4-phenylpyridinium cation (MMP+) and *N*-methyl-beta-carbolines? Biochem J 1993;291:673–6.
[35] Mizuno Y, Sone N, Saitoh T. Effects of 1-methyl-4-phenyl-1,2,3,6-tetrahydropyridine and 1-methyl-4-phenylpyridinium ion on activities of the enzymes in the electron transport system in mouse brain. J Neurochem 1987;48:1787–93.
[36] Fields JZ, Albores RR, Neafsey EJ, Collins MA. Inhibition of mitochondrial succinate oxidation—similarities and differences between *N*-methylated beta-carbolines and MPP+. Arch Biochem Biophys 1992;294:539–43.
[37] Mizuno Y. Contribution of MPTP to studies on the pathogenesis of Parkinson's disease. Rinsho Shinkeigaku 1989;29:1494–6.
[38] Desai VG, Feuers RJ, Hart RW, Ali SF. MPP (+)-induced neurotoxicity in mouse is age-dependent: evidenced by the selective inhibition of complexes of electron transport. Brain Res 1996;715:1–8.
[39] Cardellach F, Marti MJ, Fernandez-Sola J, Marin C, Hoek JB, Tolosa E, Urbano-Marquez A. Mitochondrial respiratory chain activity in skeletal muscle from patients with Parkinson's disease. Neurology 1993;43:2258–62.
[40] Bindoff LA, Birch-Machin MA, Cartlidge NE, Parker Jr WD, Turnbull DM. Respiratory chain abnormalities in skeletal muscle from patients with Parkinson's disease. J Neurol Sci 1991;104:203–8.
[41] Benecke R, Strumper P, Weiss H. Electron transfer complexes I and IV of platelets are abnormal in Parkinson's disease but normal in Parkinson-plus syndromes. Brain 1993;116:1451–63.
[42] Gu M, Cooper JM, Taanman JW, Schapira AH. Mitochondrial DNA transmission of the mitochondrial defect in Parkinson's disease. Ann Neurol 1998;44:177–86.
[43] Elkon H, Don J, Melamed E, Ziv I, Shirvan A, Offen D. Mutant and wild-type alpha-synuclein interact with mitochondrial cytochrome *c* oxidase. J Mol Neurosci 2002;18:229–38.
[44] Battino M, Littarru GP, Gorini A, Villa RF, Coenzyme Q. Peroxidation and cytochrome oxidase features after Parkinson's-like disease by MPTP toxicity in intra-synaptic and non-synaptic mitochondria from *Macaca fascicularis* cerebral cortex and hippocampus: action of dihydroergocriptine. Neurochem Res 1996;21:1505–14.
[45] Pastoris O, Dossena M, Foppa P, Catapano M, Ferrari R, Dagani F. Biochemical evaluations in skeletal muscles of primates with MPTP Parkinson-like syndrome. Pharmacol Res 1995;31:361–9.
[46] Ross NS, Hoppel CL. Acyl-CoA dehydrogenase activity in the riboflavin-deficient rat. Effects of starvation. Biochem J 1987;244: 387–91.
[47] Scholte HR, Busch HF, Bakker HD, Bogaard JM, Luyt-Houwen IE, Kuyt LP. Riboflavin-responsive complex I deficiency. Biochim Biophys Acta 1995;24(1271):75–83.
[48] Antozzi C, Garavaglia B, Mora M, Rimoldi M, Morandi L, Ursino E, DiDonato S. Late-onset riboflavin-responsive myopathy with combined multiple acyl coenzyme A dehydrogenase and respiratory chain deficiency. Neurology 1994;44:2153–8.
[49] Bakker HD, Scholte HR, Jeneson JA, Busch HF, Abeling NG, van Gennip AH. Vitamin-responsive complex I deficiency in a myopathic patient with increased activity of the terminal respiratory chain and lactic acidosis. J Inherit Metab Dis 1994;17:196–204.
[50] Armstrong Frank B. Biochemistry, 2nd ed. New York: Oxford University Press Inc.; 1983.
[51] Maublant J, Vuillez JP, Talbot JN, Lumbroso J, Muratet JP, Herry JY, Artus JC. Positron emission tomography (PET) and (F-18)-fluorodeoxyglucose in (FDG) in cancerology. Bull Cancer 1998;85: 935–50.

[52] Chesney J, Mitchell R, Benigni F, Bacher M, Spiegel L, Al-Abed Y, Han JH, Metz C, Bucala R. An inducible gene product for 6-phosphofructo-2-kinase with an AU-rich instability element: role in tumor cell glycolysis and the Warburg effect. Proc Natl Acad Sci USA 1996;96:3047–52.

[53] Baggetto LG. Deviant energetic metabolism of glycolytic cancer cells. Biochimie 1992;74:959–74.

[54] Nielsen FU, Daugaard P, Bentzen L, Stodkilde-Jorgensen H, Overgaard J, Horsman MR, Maxwell RJ. Effect of changing tumor oxygenation on glycolytic metabolism in a murine C3H mammary carcinoma assessed by *in vivo* nuclear magnetic resonance spectroscopy. Cancer Res 2001;61:5318–25.

[55] Brizel DM, Prosnitz LR, Sibley GS, Scher RL, Rosner GL, Dewhirst MW. Tumor hypoxia adversely affects the prognosis of carcinoma of the head and neck. Int J Radiat Oncol Biol Phys 1997;38:285–90.

[56] Robinson SP, Howe FA, Stubbs M, Griffiths JR. Effects of nicotinamide and carbogen on tumour oxygenation, blood flow, energetic and blood glucose levels. Br J Cancer 2000;82:2007–14.

[57] Alagoz T, Buller RE, Anderson B, Terrell KL, Squatrito RC, Niemann TH, Tatman DJ, Jebson P. Evaluation of hyperbaric oxygen as a chemosensitizer in the treatment of epithelial ovarian cancer in xenografts in mice. Cancer 1995;75:2313–22.

[58] Abi-Saab WM, Maggs DG, Jones T, Jacob R, Srihari V, Thompson J, Kerr D, Leone P, Krystal JH, Spencer DD, During MJ, Sherwin RS. Striking differences in glucose and lactate levels between brain extracellular fluid and plasma in conscious human subjects: effects of hyperglycemia and hypoglycemia. J Cereb Blood Flow Metab 2002;22:271–9.

[59] Matsubara K, Senda T, Uezono T, Awaya T, Ogawa S, Chiba K, Shimizu K, Hayase N, Kimura K. L-Deprenyl prevents the cell hypoxia induced by dopaminergic neurotoxins, MPP(+) and beta-carbolinium: a microdialysis study in rats. Neurosci Lett 2001;302:65–8.

[60] Shulman RG, Hyder F, Rothman DL. Lactate efflux and the neuroenergetic basis of brain function. NMR Biomed 2001;14:389–96.

[61] Goodman JC, Valadka AB, Gopinath SP, Uzura M, Robertson CS. Extracellular lactate and glucose alterations in the brain after head injury measured by microdialysis. Crit Care Med 1999;27:1965–73.

[62] Fellows LK, Boutelle MG, Fillenz M. Physiological stimulation increases non-oxidative glucose metabolism in the brain of the freely moving rat. J Neurochem 1993;60:1258–63.

[63] Shishido F, Uemura K, Inugami A, Tomura N, Higano S, Fujita H, Sasaki H, Kanno I, Murakami M, Watahiki Y, Nagata K. Cerebral oxygen and glucose metabolism and blood flow in mitochondrial encephalomyopathy: a PET study. Neuroradiology 1996;38:102–7.

[64] Mazzio E, Soliman KFA. The role of glycolysis and gluconeogenesis in the cytoprotection of neuroblastoma cells against 1-methyl 4-phenylpyridinium ion toxicity. Neurotoxicology 2003;24:137–47.

[65] Nath S. The molecular mechanism of ATP synthesis by F1F0-ATP synthase: a scrutiny of the major possibilities. Adv Biochem Eng Biotechnol 2002;74:65–98.

[66] Leyva JA, Bianchet MA, Amzel LM. Understanding ATP synthesis: structure and mechanism of the F1-ATPase. Mol Membr Biol 2003;20:27–33.